The Lamellar Distribution in Isotactic Polypropylene Modified by Nucleation and Processing

Anna Romankiewicz, Tomasz Sterzynski

Poznan University of Technology, Polymer Group, PL 60-965 Poznan, Poland

Summary: An isotactic polypropylene was modified with specific α - phase and β - phase nucleation agents. The modification by processing during extrusion was realised by means of molten state elongation with various stretching ratios λ between 7.11 and 1.67. The lamellar thickness distribution was evaluated for non - elongated and elongated samples using the DSC melting curves, by an application of the general Thomson - Gibbs equation. A significant influence of heterogeneous nucleation on the lamellar distribution was confirmed. The morphological effects are visible as a shift of the maxima of the lamellar distribution and as the elongation and nucleation dependent appearance of lamellae with smaller (below 12 nm) and bigger (above 25 nm) thickness.

Introduction

The lamellae are the structural elements produced by growth of a three dimensional order during cooling of melt of semi crystalline polymers. The fold - chain fibrils forming the lamellae are produced by a radial growth of crystal systems, with less or more small - angle branching of fibrils [1-3]. Bigger units like spherulites may be found in most of semi crystalline polymers, especially, in polymers characterized by lower crystal growth rate such as polypropylene (ca. 20 μm/min), or polyethylene oxide (200 μm/min) but also in polyethylene (growth rate >1000 μm/min) [4,5]. Usually the thickness of the lamellae is of the order of about 10 nm, but by an isothermal crystallisation an overlaid of single lamellae may create the lamellae packs with a thickness of about 100 nm. If the thickness exceeds 1 μm the lamellae may be observed directly by means of the optical microscopy [6].

Depending on the polymer chemical structure and the macromolecular mobility, within the structure unit, two direction of fold - chain fibril growth: radial [R] and tangential [T] may usually be observed. For all semi crystalline polymers the lamellae thickness presents a considerable dependence on the crystallisation conditions, especially on the crystallisation temperature and the annealing time. For a sufficient high temperature and

 CCC 1022-1360/00/$ 17.50+.50/0

time the lamellar thickness may increase even ten times [7-9] comparing with low temperature and non-isothermal crystallization conditions.

The nature of the lamellar morphology may usually be directly observed by polarised light optical microscopy (MPO) or by scanning electron microscopy (SEM). The average lamellar thickness may be detected by means of small angle X - ray scattering (SAXS) [6] or by the differential scanning calorimetry (DSC) [10-14]. In the case of SAXS measurements, the position of the maximum on the diffraction curve $Is^2 = f(s)$, where I is the diffraction intensity and s - the scattering vector, allows to evaluate the average value of the long period, i.e. the distance between two crystalline layers in a multi-layer lamella model. By the DSC measurements the lamellar thickness l may be estimated using of the Thomson - Gibbs relationship.

Lamellar Thickness by DSC

For this procedure a hypothesis relating the lamellae distribution to the form the DSC curve $\Delta H = f(T)$ is taken into account [10-13]. It is known that the temperature affects the crystallisation kinetics, and from other side the lamella thickness affects the melting point of the polymer crystals. This relationship was expressed in a form of the Thomson-Gibbs equation [14]:

$$T_m = T_m^0 \left(1 - \frac{2\sigma_e}{l \Delta H_f} \right) \qquad (1)$$

where:

T_m - melting temperature of the investigated polymer,

T_m^0 - the equilibrium melting temperature,

l - the lamella thickness (longitudinal dimensions of the crystal),

ΔH_f - the melting enthalpy of a perfect crystal,

σ_e - free surface energy of the end faces at which chains fold.

The thickness distribution of the crystalline lamellae, related to the DSC thermograms, may be expressed by the following equation:

$$f(l) = \frac{1}{M} \frac{dM}{dl} \qquad (2)$$

where the lamella thickness of a polymer is related to the melting temperature T_m of a single crystal by the equation:

$$l = \frac{2\sigma_e T_m^0}{\Delta H_f \left(T_m^0 - T_m\right)} \qquad (3)$$

and

$$dM = \frac{dE}{dT}\frac{dT}{\Delta H_f}\rho_c \qquad (4)$$

where:

ρ_c - the density of the crystal phase,

dE - the energy necessary to melt the crystalline mass dM in the temperature range between T and $T+dT$.

From eq. (3) and (4) follows:

$$\frac{dM}{M} = \frac{dE}{dT}\frac{dT}{\Delta H_f M}\rho_c \qquad (5)$$

where the temperature increase:

$$dT = dl\frac{\left(T_m^0 - T_m\right)^2}{T_m^0}\frac{\Delta H_f}{2\sigma_e} \qquad (6)$$

and the thickness distribution may be expressed as follows:

$$\frac{1}{M}\frac{dM}{dl} = \frac{dE/dT\left(T_m^0 - T_m\right)^2 \rho_c}{2\sigma_e T_m^0 M} \qquad (7)$$

The evaluation of the following equation is based on the DSC measurements:

$$\frac{dE}{dT}\frac{1}{M}\left[\frac{J}{^{\circ}C}\frac{1}{kg}\right] = Heat.Flow\left[\frac{J}{kg\cdot\min}\right] / V_{cooling.or.heating}\left[\frac{^{\circ}C}{\min}\right] \qquad (8)$$

The *Heat Flow* is the value of the ordinate on the original DSC curve with subtracted base line. The parameters for the description of the crystallization of the monoclinic (α-form) and hexagonal (β-form) of an isotactic polypropylene, according to [15-17], are presented in Table 1.

Table 1. The parameters characterizing the crystallization of α-iPP and β-iPP.

	T_m^0 [K]	ΔH_f [J/cm^3]	σ_e [J/cm^2]	ρ_c [g/cm^3]
α-phase iPP	464.0[14]	196[14]	102.9[14]	0.936[15]
β-phase iPP	449.2[16]	177[16]	55.2[16]	0.921[15]

Experimental Part

Material

A commercial iPP NOVOLEN 1100H, produced by BASF (Germany), was used in this study. The density is 910 kg/m^3 and the melt flow rate (MFI 230°C, 2.16 kg) = 2.4 cm^3/ 10 min.

Nucleating agents: 1, 3: 2, 4 – bis (3, 4-dimetylobenzylideno) sorbitol (DMDBS) (Milliken, Belgium), with melting point T_m =277°C and crystallization temperature T_{cr} = 214°C, was applied as a specific α nucleating agent, and N, N' – dicykloheksylo – 2, 6 – naftaleno dikarboksy amide (NJ), (Palmarole Ltd, UK) with melting point T_m = 387°C and crystallization temperature T_{cr} = 137°C, as a β - form nucleate.

Sample preparation

The nucleates were mixed with the pallets via powder sprinkling on the surface of the granules. The homogenization was performed using a single screw extruder FAIREX (ϕ = 30 mm and L/D = 24) operating at the barrel temperatures of 25°C, 140°C, 180°C, 185°C, and the die at 195°C and 190°C, respectively. The screw rotation speed was 30 rpm. A powder mixing and molten state extrusion was used to prepare two master batches containing 0.5 wt. % of both, the α- phase (DMDBS) and β- phase (NJ) nucleating agents. This procedure was succeed by solution of the master batch with pure iPP, with the aim to achieve the concentration of nucleating agents (NA's) in the range from 0.001 wt. % to 0.5 wt. %.

For a better distribution of the NA's in the iPP matrix, a double melting mixing procedure was applied for each composition.

Molten state elongation

The molten state elongation was completed between the extrusion die and the entrance to the cooling device, by means of a profile extrusion with a flat die 2 x 20 mm, and a pulling device operating with various drawing rates. By variation of the pulling rate, stretching ratios (λ) of the profile between λ = 1.67 and λ = 7.11 was achieved.

Differential scanning calorimetry (DSC)

For the thermal characterization of the polymeric materials the DSC Netzsch 200

thermal analysis system was used. The average weight of the samples was between 5 and 8 mg. Following DSC temperature program was applied: first heating, in the range from 30°C to 200°C, with a rate of 10°C min^{-1}, maintenance at this temperature for 5 min, cooling to 40°C with a cooling rate of 5°C min^{-1}, maintenance at 40°C during 5 minutes and second heating up to 200°C with a rate of 10°C min^{-1}.

For all specific nucleated and elongated iPP samples following parameters were determined: the melting temperature T_m, the crystallization temperature T_{cr} as well the temperature dependent heat of fusion ΔH_f (shape of the DSC first melting curve). As the aim of these studies was to relate the iPP lamella structure to the nucleation and processing history, the evaluation of the lamellar distribution was performed always for the first DSC melting curve. For comparison, also samples without nucleation, neither elongation were examined.

It is known that the first heating scan of a DSC is affected by many errors, which can significantly influence the reported results. The most important is the heat exchange coefficients between sample and holder, as well between holder and oven [18]. In order to minimize this error and to assure an adequate heat flow, each of samples were flat adhered to the DSC pans.

To examine the structure of polypropylene modified by nucleation and processing, the DSC samples were taken through the whole thickness of the film, in the middle of flow. On this way the results may be comprehend as typical mean values of processing and nucleation induced iPP structure modification. In order to minimize the measurement error and to determinate the average value of T_m and ΔH_f the DSC melting procedure, performed always in the same conditions, was repeated for a number of samples. We have observed an adequate repetition of the DSC results, e.g. of the melting temperature and of the corresponding enthalpy.

Results

DSC melting curves

The DSC melting process by an isotactic polypropylene may be strongly influenced as well by the thermal and mechanical history [19] as by the composition of the polymeric system. Even a very low content of specific nucleating agents may significantly modify the DSC melting curve, as it was already shown in the case of quinacridone and other additives [4,5,20,21]. Same results were attained in the reported case where the β - phase in

iPP was produced by the addition of NJ [22,23].

The following curves reveal to iPP modified by heterogeneous nucleation with various content of the specific nucleating agents, produced by an extrusion homogenization and following palletizing. The DSC melting curves for the iPP nucleated with DMDBS are presented on Figure 1.

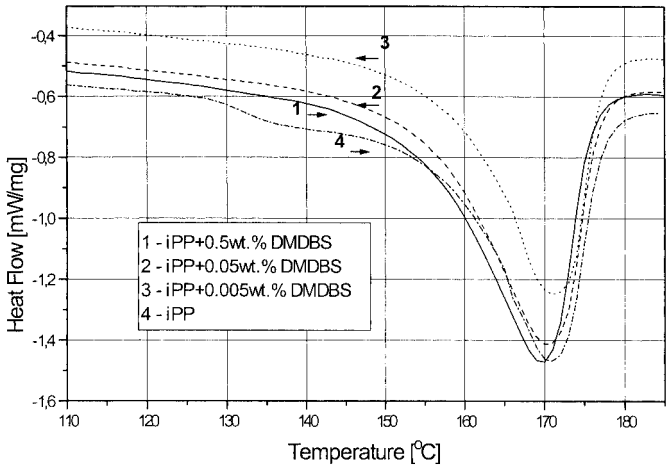

Figure 1. The melting curves of iPP nucleated with DMDBS.

The melting curves for the iPP nucleated with DMDBS present almost the same shape for all compositions, independent on the quantity of the nucleating agent added. On Figures 2 and 3 the DSC melting curves for the iPP nucleated with various content of NJ are shown where the curves on Figure 2 correspond to the first melting and on Figure 3 to the second melting.

The comparison of values of T_m and ΔH_f for iPP without and with different content of nucleating agents is presented in Table 2. A small shift of melting temperature observed by DSC first melting run may be related to somehow modified thermal stability of various samples or/and to certain measurement error [18], a problem which was already discussed before.

The difference in the run of the DSC curves in both cases may be related to various cooling conditions. The DSC melting curves presented on Figure 2 were recorded for rapidly cooled samples, produced by molten state extrusion followed by palletizing and

content of the β-form reached values of about 99%, for the NJ concentration of 0.5 wt.%.

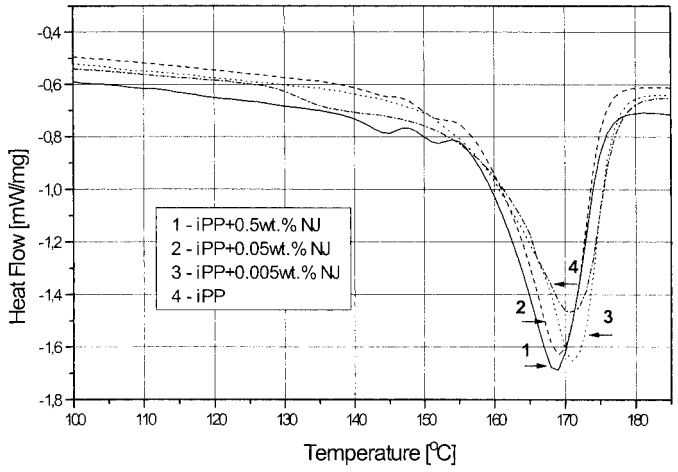

Figure 2. The melting curves of iPP with NJ (first melting).

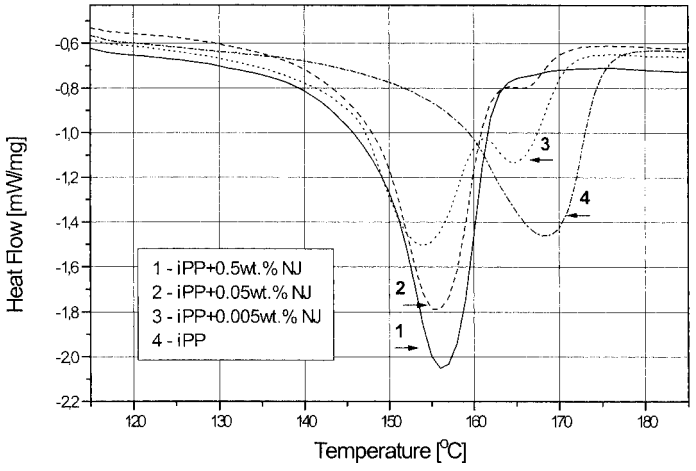

Figure 3. The melting curves of iPP nucleated with NJ (second melting).

The following results reveal to samples produced by melt stretching in an extrusion process. The DSC melting curves for non-nucleated and nucleation modified iPP samples, processed with various molten state stretching ratios, are shown on Figures 5

content of the β-form reached values of about 99%, for the NJ concentration of 0.5 wt.%.

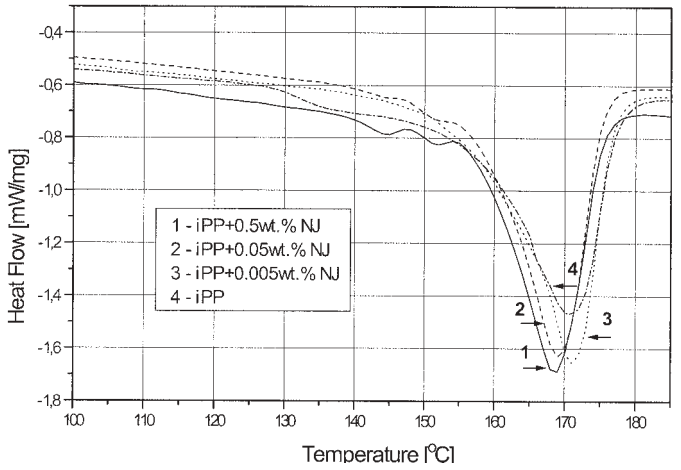

Figure 2. The melting curves of iPP with NJ (first melting).

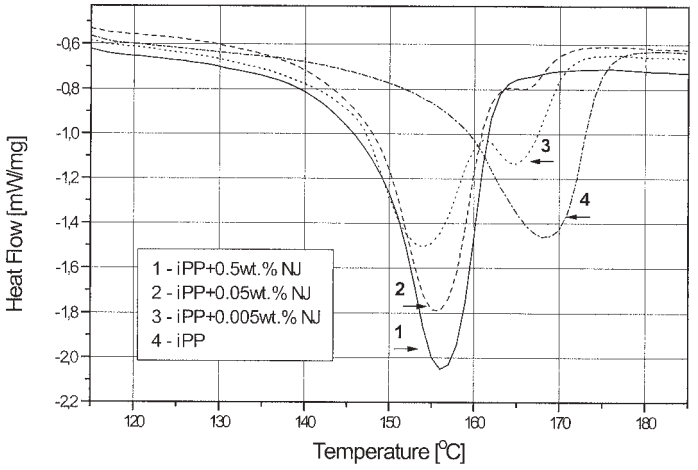

Figure 3. The melting curves of iPP nucleated with NJ (second melting).

The following results reveal to samples produced by melt stretching in an extrusion process. The DSC melting curves for non-nucleated and nucleation modified iPP samples, processed with various molten state stretching ratios, are shown on Figures 5

to 7. As it may be seen a higher elongation ratio leads to a duplication of the maximum, an effect that may indicate an elongation dependent creation of a bi - modal lamellar thickness distribution.

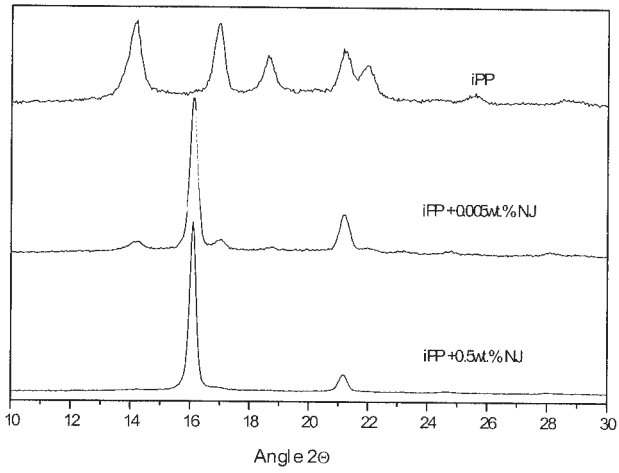

Figure 4. The WAXS patterns of iPP "pure" and with NJ.

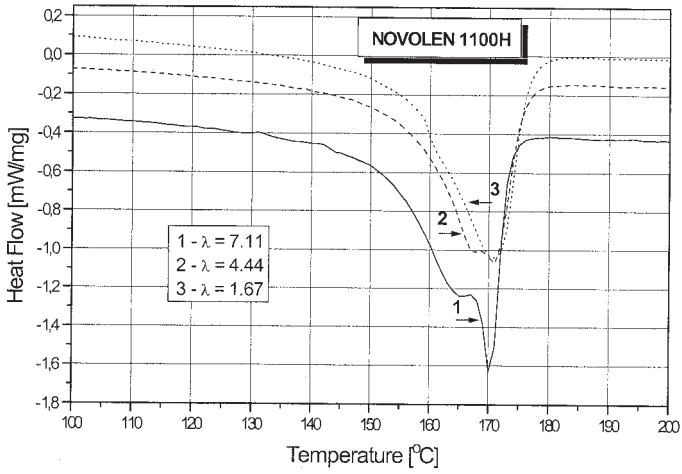

Figure 5. The melting curves of non-nucleated iPP samples processed with different λ.

The stretching ratio applied in this study led to different orientation degree in extruded products, as determined by FTIR spectroscopy [23].

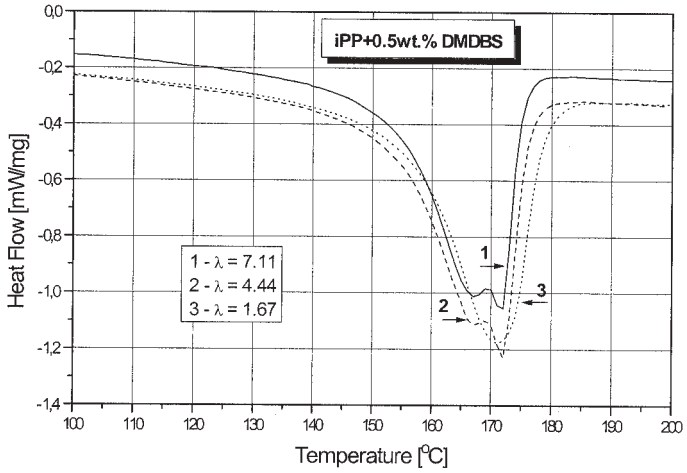

Figure 6. The DSC melting curves of iPP samples nucleated with DMDBS and processed with different stretching ratios.

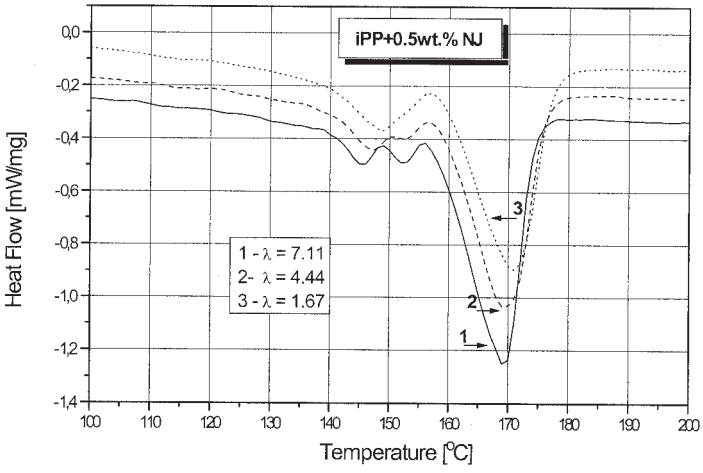

Figure 7. The melting DSC curves of iPP nucleated with NJ and processed with different stretching ratios.

Nucleation dependent lamellar distribution

The lamellar distribution function $f(l) = \frac{1}{M}\frac{dM}{dl}$, for various compositions of iPP samples and elongation ratios, are presented on Figures 8 to 12. For the estimation of

the nucleation dependent lamellar distribution only the equilibrium temperature for the monoclinic iPP was taken into account, as the performance of the DSC peak separation for the α/β phase iPP isn't convinced. Therefore, the comparison of the lamellar distribution, for samples produced the by varied nucleating agent content and by various melt stretching, was achievable. On Figure 8 the lamellar distribution for pure iPP and iPP with 0.5 wt. %, 0.05 wt. % and 0.005 wt. % of DMDBS (α - phase nucleating agent) is presented.

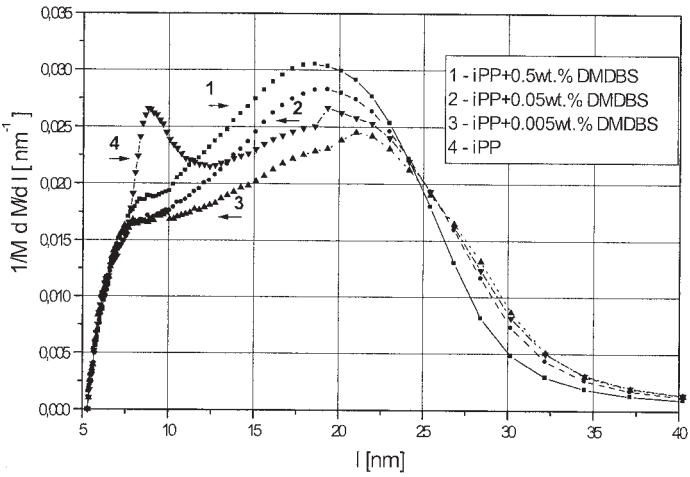

Figure 8. The lamellar distribution for pure iPP and iPP with 0.5 wt. %, 0.05 wt. % and 0.005 wt. % of the DMDBS.

The changes of the concentration of the nucleating agent lead to certain modification of the lamellar distribution. In this case two effects may be observed and discussed separately, a shift of the maximum corresponding to the most probable lamella value, and the existence of bigger lamellae with an average value above 25 nm. As it follows from figure 8, an increase of the DMDBS content leads to somehow lower average lamellae values, (maximum at about 22 nm for 0.005 wt. % and at about 18 nm for 0.5 wt. %) and more homogeneous lamellar distribution, e.g. a much smaller participation of bigger lamellae, over 25 nm. This kind of concentration dependent lamellae distribution may be compared to the relationship between the modification of the crystallization temperature T_{cr} and the DMDBS content, where a similar influence of the DMDBS content on the T_{cr} was found [23].

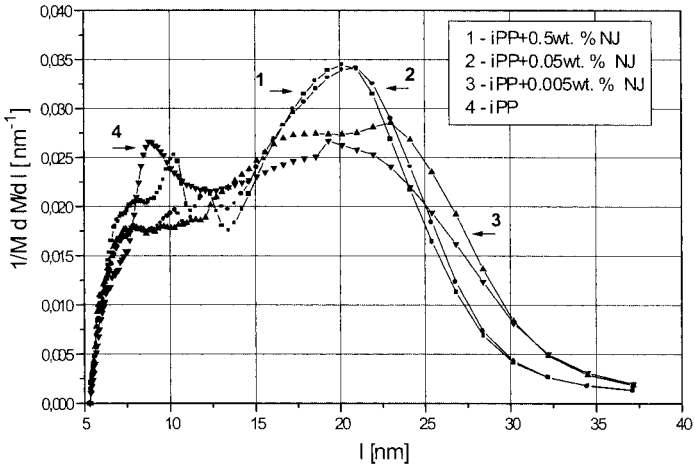

Figure 9. The lamellar distribution for pure iPP and iPP with 0.5 wt. %, 0.05 wt. % and 0.005 wt. % of NJ.

For the iPP with the β - phase nucleating agent - NJ (Figure 9) similar observation, as for iPP modified with DMDBS, may be done (for comparison the lamellar distribution was evaluated based on the first melting DSC curve). A concentration dependent shift of the maximum towards lower lamellae values and a clear change in the form of the curve, with a significant part of higher lamellae values (about 25 nm), for the lowest NJ-content, was noted. This kind of relationship may also be attributed to the NJ - concentration dependent changes of the crystallization temperature - T_{cr}, where even a low NJ-content leads to a significant increase of T_{cr} - an effect which was already observed and confirmed in our research [22,23]. Additionally, a certain amount of smaller lamellae, with average values between 7 and 15 nm, may be attributed to the considerable β - phase existence in these iPP samples (the content of the hexagonal phase determined by WAXS was between 89 and 99% [23]).

For comparison with presented results also an isothermal crystallization of "pure" iPP samples by 122°C, 124°C, and 127°C was realized by the DSC procedure. A satisfactory agreement of the lamellar distribution for an isothermal crystallization with curve 4 on Figure 9 was found.

Molten state elongation induced modification of the lamellar distribution

On following figures the influence of molten state stretching on the lamellar distribution, in iPP samples without and with nucleating agents, is presented. The curves on Figure10 represent the lamellar distribution of "pure" iPP elongated with various stretching ratios λ.

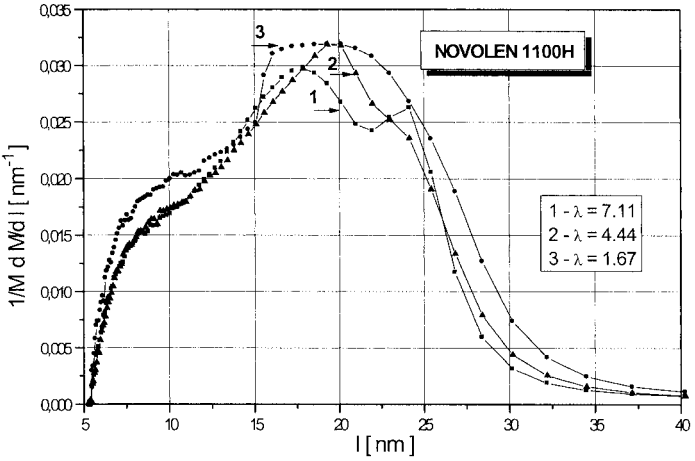

Figure 10. The lamellar distribution of pure iPP elongated with various stretching ratios λ.

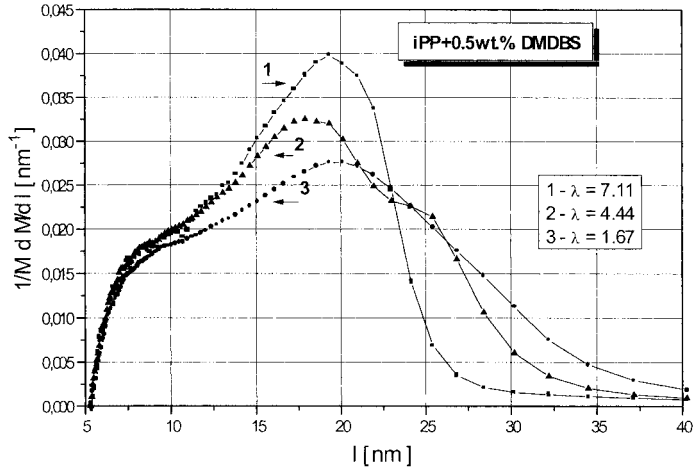

Figure 11. The lamellar distribution for iPP with 0.5 wt. % of DMDBS elongated with various stretching ratios λ.

For the highest λ - value by uni-axial elongation of "pure" iPP a relative homogeneous lamellar distribution, with a bimodal distribution may be observed. On the contrary, a rather uniform curve in the middle part, with somehow bigger part of broaden lamellae, over 25 nm, was noted if a lower stretching ratio (λ = 1.67) was applied.

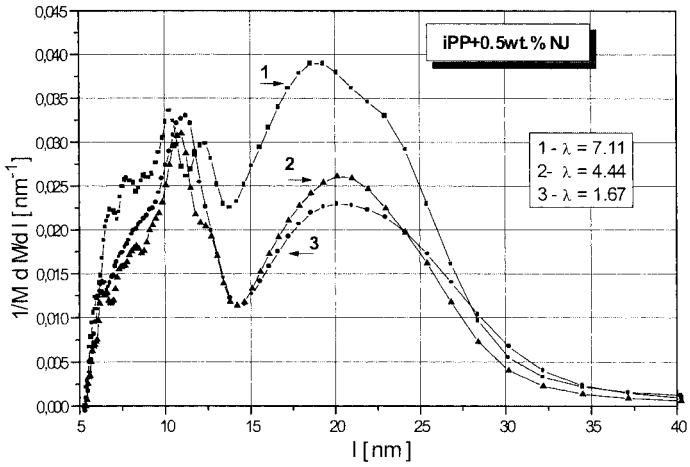

Figure 12. The lamellar distribution for iPP with β -phase nucleating agent, stretching ratios λ = 1.67, 4.44 and 7.11.

With increasing stretching ratio λ. a more narrow run of the lamellar distribution function may be observed for the specific α - nucleated iPP samples (Figure 11). For the stretching ratio λ = 7.11 the distribution function $f(l) = \frac{1}{M}\frac{dM}{dl}$ presents a smooth curve with a clear maximum for l = 20 nm. On the contrary, for lower uni – axial deformation the lamellar distribution is much broader, with a bimodal distribution for λ = 4.44. The lamellae with a mean thickness above 25 nm are observed only for lower stretching ratios. Figure 12 presents the distribution function (equation 2) for the iPP samples nucleated with β -phase nucleating agent and elongated to λ = 1.67, 4.44 and 7.11. Similar, like in Figure 11, a significant maximum for the highest stretching ratio was observed, where for lower λ a fewer developed maximum of the lamellar distribution function for β – nucleated iPP may be noted. For this type of iPP modification also a significant participation of lamellae with mean thickness values in the range between l = 7 nm and l = 12 nm, related to the existence of β - phase lamellae

may be observed. The probably reasons for the change of the average lamella value are:

- dependent of the crystallization ratios on the specific nucleation of iPP, or/and
- temperature dependent increase of crystal growth of monoclinic and hexagonal phase of iPP in defined temperature range [5].

Conclusions

A significant influence of the heterogeneous nucleation on the lamellar distribution in the iPP samples, deformed uni-axial in a molten state, was confirmed. The changes of the lamellar distribution function may be attributed to the nucleation-induced modification of the crystallization kinetics. In relationship with molten state processing, the use of specific additives (nucleating agents) plays a dominating role as well by the changes of the germination density, as by the creation of various lamellae types and by modification of its radial growth ratio.

Acknowledgement

Project partly supported by Polish Research Committee KBN 7.T08E.047.17

References

[1] B. Wunderlich, *Macromolecular Physics,* Academic Press, New York (1973).
[2] D. Trifonova, J. Varga and G. J. Vancso, *Polymer Bulletin*, 41, (1998), p. 341.
[3] H.-G. Elias, *Macromolecules 1, Structure and Physics,* Plenum Press, New York (1984).
[4] J. Varga, *J. Thermal Analysis*, 35, (1989), p. 1891.
[5] J. Varga, *J. Mater. Sci.*, 27, (1992), p. 2557.
[6] T. Sterzynski, "*Lamella dimension and distribution*", [in:] *Polypropylene: an A-Z*, Ed. J. Karger-Kocsis, Kluwer Academic Publisher, Dordrecht (1999), p. 374.
[7] K. Yamada, S. Matsumoto, K. Tagashira and M. Hikosaka, *Polymer*, 39, (1998), p. 5327.
[8] M. Aboulfaraj, B. Ulrich, A. Dahoun and C. G'sell, *Polymer*, 34, (1993), p. 4817.
[9] T. Sterzynski, P. Calo, M. Lambla and M. Thomas, *Polym. Eng. Sci.*, 37, (1997), p. 1.
[10] Y. L. Huang and N. Brown, *J. Polym. Sci.*, 29, (1991), p.129.
[11] M. Alonso, J. C. Rodriguez – Cabello, J. C. Merino and J. M. Pastor, *Macromol. Chem. Phys.*, 197, (1996), p. 3269.
[12] C. J. G. Plummer and H.-H. Kausch, *Polymer Bulletin*, 36, (1996), p. 355.
[13] J. C. Rodriguez – Cabello, M. Alonso, J. C. Merino and J. M. Pastor, *J. Appl. Polymer Sci.*, 60, (1996), p. 1709.
[14] V. A. Bershtein and V. M. Egorov, *Differential Scanning Calorimetry of Polymers. Physics, Chemistry, Analysis,* Ellis Horwood, London (1994).
[15] Z. Bartczak and A. Galeski, *Polymer,* 31, (1990), p. 2027.
[16] J. Karger – Kocsis, J. Varga and G. W. Eherenstein, *J. Appl. Polymer Sci.*, 64, (1997), p. 2057.
[17] G. Shi, X. Zhang and Z. Qiu, *Makromol. Chem.*, 193, (1992), p. 583.
[18] G.Eder, H.Janeschitz-Kriegl, The Polymer Processing Society, Ninth Annual Meeting, Manchester (1993) p. 452
[19] T. Sterzynski, H.Oyased, to be published

[20] J. Varga, *J. Thermal Analysis*, 31, (1986), p. 165.
[21] T. Sterzynski, M. Lambla, F. Georgi and M. Thomas, *Intern. Polymer Processing XII*, 1, (1997), p. 64.
[22] A. Romankiewicz and T. Sterzynski, *World Polymer Congress IUPAC* MACRO 2000, Warsaw (2000) p. 966.
[23] A. Romankiewicz, Phd Thesis, Poznan University of Technology, Poznan 2001.
[24] B. Fillon, A Thierry, J. C. Wittmann and B.Lotz, *J. Polymer Sci., Part B, Polymer Phys.*, 31, (1993), p. 1407.